Estimation Strategy for a Series of Grinding Cycles in Batch Production

Cheol W. Lee

***Abstract*—Typical grinding operations in batch production are characterized by multiple data streams sampled at distinct intervals. A unique estimation strategy is proposed for integrating rapidly sampled sensor signals with postprocess inspection data from a series of grinding cycles. After a nonlinear state-space model is derived from existing analytical models, system observability is tested for various combinations of sensors and measurement settings. A multirate simultaneous state and parameter estimation scheme is developed based on extended Kalman filters for real-time estimation of the model parameters and part quality. Results from case studies demonstrate that the proposed scheme enables challenging estimation tasks to be undertaken that cannot be performed using traditional approaches.**

***Index Terms*—Batch production, control, grinding, machining, monitoring, multirate, observer.**

I. Introduction

THE grinding process accounts for approximately 30% of the total expenditure associated with manufacturing a precision part. However, the grinding process remains one of the most complex and difficult-to-control manufacturing processes due to its complex, nonlinear, and stochastic nature. Controlling and monitoring the grinding process is further hampered by the considerable difficulty of obtaining real-time feedback about the qualities of a part, such as its surface finish and roundness.

The difficulties of in-process measurement of part quality have led to active research into its estimation based on real-time sensing of easy-to-measure process variables such as the grinding power, acoustic emission, and the vibration. Various techniques have been used to identify links between the signals from such sensors and part quality, including sensor fusion and clustering. An extensive review on such methods for machining operations is given in [1]. Although valuable information on part quality is available from inspections in most manufacturing plants, none of the existing approaches fully utilize the available data. The scheme proposed here is one of the first attempts to use both real-time signals and postprocess measurement data to estimate consecutive grinding cycles in an autonomous manner.

Lee recently derived a state-space model for the grinding process by converting dynamic relationships in existing analytical models into a state-space equation, which allows both the part quality and sensor output to be represented as static functions of the state and input variables [2]. The state-space model structure naturally enables an observer to be designed for real-time estimation of the part quality from the sensor output. Several observer-based approaches have been successfully applied to estimating the tool conditions in machining operations [3], [4].

A necessary condition for using an observer in a grinding process is full observability of the grinding system. A system is observable if every state can be determined from the observation of available output variables over a finite time interval. A preliminary analysis of the observability for various measurement settings showed that the grinding process is often rendered unobservable for certain estimation tasks [2]. A lack of observability is more common when attempting to account for any model-process mismatch by estimating both the model parameters and the state variables. A basic idea in this paper is to improve observability by supplementing in-process sensor signals with postprocess measurement of the part quality from previous cycles. It is expected that the systematic utilization of the postprocess measurement data in this way will significantly improve the estimation performance for grinding systems in batch production. We first explain multirate data flows from a series of grinding cycles, and then derive a state-space model based on various grinding models reported in the literature. An observability test is performed, and then the proposed estimation scheme is presented. Simulations with two case studies on estimating a series of grinding cycles are then described.

II. Modeling of Grinding Cycles in Series

A. Data Flows From Batch Production

Batch production is commonly employed in industry to manufacture a group of parts or products with identical design and specifications. The start of a new batch is marked by the launch of a new design, tool change, or arrival of a new lot from suppliers or preceding processes. From a control point of view, the start of a new batch normally coincides with significant changes in the process dynamics, and hence it is necessary to update the states and model parameters as early as possible when a new batch starts. Fig. 1 shows a schematic of batch production when N parts are processed in series on a grinding machine.

Many machine tools in modern industry are equipped with various sensors for monitoring process variables such as the grinding power, which are generally sampled at a constant frequency. In contrast, the quality of each part is usually only measured at a postprocess inspection after its grinding cycle is completed. Ignoring the idle time between two consecutive grinding cycles, a series of grinding operations can be viewed as a continuous process with two output streams sampled at two distinct intervals. In this paper, the sampling time of the sensor signal (T_f) is set constant, and that of the part quality is $T_i(> T_f)$,

Manuscript received September 12, 2006; revised March 2, 2007. Manuscript received in final form June 18, 2007. Recommended by Associate Editor S.-L. Jásmá-Jounela. This work was supported in part by the University of Michigan-Dearborn under a Faculty Summer Research Grant and the University of Michigan under the Office of the Vice President for Research (OVPR) Grant.

The author is with the Industrial and Manufacturing Systems Engineering, University of Michigan-Dearborn, Dearborn, MI 48128 USA (e-mail: cheol@umich.edu).

Color versions of one or more of the figures in this paper are available online at http://ieeexplore.ieee.org.

Digital Object Identifier 10.1109/TCST.2007.908225

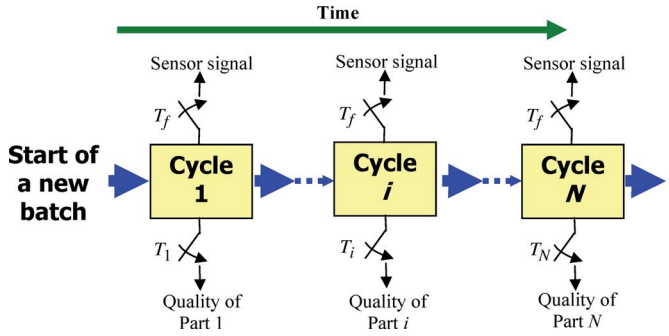

Fig. 1. Two data streams from the grinding process in a batch production.

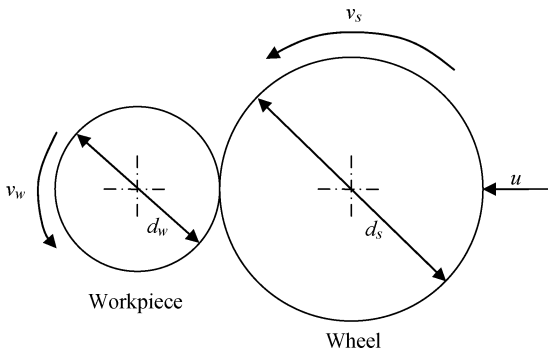

Fig. 2. Configuration of a cylindrical plunge grinding process.

which corresponds to the cycle time of the ith grinding cycle, as shown in Fig. 1.

B. Derivation of a State-Space Model

The derivation of a state-space model from existing analytical models of the cylindrical plunge grinding process is briefly described here (a more detailed derivation can be found in [2]). Fig. 2 shows a schematic of a cylindrical grinding process, in which a rotating cylindrical workpiece with a nominal diameter of d_w and a surface velocity of v_w is ground by a rotating grinding wheel with a nominal diameter of d_s and a surface velocity of v_s. The grinding wheel is fed into the workpiece at a command infeed rate u.

Three dynamic relationships are included for the cylindrical grinding process in analytical models in the literature. It is assumed that the grinding is carried out in a chatter-free region. The first relationship is the dynamic delay of the actual infeed rate, v (mm/s), in response to the command infeed rate, u (mm/s), due to the mechanical stiffness and sharpness of the wheel surface, which is frequently modeled as a first-order system [5], [6]

$$\dot{v} = (u - v)/\tau \tag{1}$$

where τ (s) is the time constant whose value is dependent on the machine-wheel-workpiece stiffness and the sharpness of the wheel. The sharpness of the wheel decreases with the accumulated amount of material removed after a tool change, V'_w (mm^3/mm), due to attrition of the grits [6]. The accumulated metal removal, by its definition, is related to infeed rate v by another first-order differential equation

$$\dot{V}'_w = \pi d_w v. \tag{2}$$

On the other hand, the radial wheel wear—which involves a progressive reduction in the diameter of the grinding wheel—is obtained by manipulation of analytical models in the literature [2], [7] as

$$\dot{d}_s = -\frac{2\pi^g d_w^{1+g}}{d_{s_0} G_1} v_s^{-g} v^{1+g} \tag{3}$$

where d_{s_0} is the initial wheel diameter (mm), and G_1 and g are model parameters.

Based on (1)–(3), three state variables are defined to describe the dynamic relationships in the grinding process using the following state equation:

$$\dot{\mathbf{x}} = \mathbf{f}(\mathbf{x}, \mathbf{u}) + \boldsymbol{\eta}(t) \tag{4}$$

where $\mathbf{x} = (x_1, x_2, x_3)^{\mathrm{T}} = (V'_w, v, d_s)^{\mathrm{T}} \in \Re^3$, $\mathbf{u} = (u_1, u_2)^{\mathrm{T}} = (u, v_s)^{\mathrm{T}} \in \Re^2$, and $\boldsymbol{\eta}(t) \in \Re^3$ are the state vector, input vector, and process noise, respectively, and $\mathbf{f}$ is a nonlinear vector function.

It was shown in [2] that many existing models for the outputs from a grinding process can be converted into static functions of the state and input variables. Appendix A provides the output equations derived from the literature for various outputs such as the grinding power, roundness, part-size reduction, surface roughness, and wheel diameter. The output equation of the state-space model can be written as

$$\mathbf{y} = \mathbf{h}(\mathbf{x}, \mathbf{u}) + \boldsymbol{\xi}(t) \tag{5}$$

where $\mathbf{y}$ is the output vector, $\boldsymbol{\xi}(t)$ is the measurement noise, and $\mathbf{h}$ is a nonlinear vector function. According to the two distinct sampling intervals described in Section II-A, the output vector can be divided into a fast-measurement vector $\mathbf{y}_f$ and a slow-measurement vector $\mathbf{y}_s$ (i.e., $\mathbf{y} = [\mathbf{y}_f; \mathbf{y}_s]$). The components of $\mathbf{y}_f$ are real-time sensor signals of the grinding power and part-size reduction, whereas those of $\mathbf{y}_s$ correspond to the roundness, surface roughness, and wheel diameter, which are measured through postprocess inspection.

As in many adaptive filtering schemes, the model parameters are modeled as the random walk processes and then appended to the state vector to form an augmented system

$$\dot{\mathbf{X}} = \mathbf{F}(\mathbf{X}, \mathbf{u}) + \boldsymbol{\eta}_1(t) \tag{6}$$

where $\mathbf{X}$ equals $[\mathbf{x}; \boldsymbol{\theta}]$; $\boldsymbol{\eta}_1(t)$ corresponds to $[\boldsymbol{\eta}(t); \boldsymbol{\upsilon}(t)]$, where $\boldsymbol{\eta}(t)$ and $\boldsymbol{\upsilon}(t)$ are white Gaussian noises, and $\boldsymbol{\theta}$ is the vector of model parameters whose dynamics is given as $\dot{\boldsymbol{\theta}} = \boldsymbol{\upsilon}(t)$. The output equation can be represented using the augmented state vector

$$\mathbf{y} = \mathbf{H}(\mathbf{X}, \mathbf{u}) + \boldsymbol{\xi}(t). \tag{7}$$

TABLE I
OBSERVABILITY UNDER VARIOUS CONDITIONS

Case	Variables to be estimated		Measurement setting		Observability
	State variables	Model parameters	In-process sensors	Postprocess inspection	
1	x_1, x_2, x_3	-	P, D_w	-	Deficient
			P	d_s	Full
2	x_1, x_2, x_3	R_0	P, D_w	d_s	Deficient
			P	d_s, R_a	Full

C. Discrete-Time Representation

The augmented system in (6) is represented in the discrete-time domain as follows:

$$\mathbf{X}(i, j+1) = \mathbf{F}_d\left[\mathbf{X}(i, j), \mathbf{u}(i, j)\right] + \boldsymbol{\eta}_1(i, j) \tag{8}$$

where $\mathbf{X}(i, j)$ denotes the state vectors at the jth sampling instance of the ith grinding cycle, $i(= 1, 2, \ldots, N)$ denotes the cycle number, $\boldsymbol{\eta}_1(i, j)$ is the white Gaussian noise sequence (whose covariance is $\mathbf{Q}$), and $\mathbf{F}_d(\mathbf{X}, \mathbf{u}) = \mathbf{X} + T_f\mathbf{F}(\mathbf{X}, \mathbf{u})$. Assuming the cycle time of the ith cycle T_i is given by n_i (an integer) times the sampling time T_f (i.e., $T_i = n_i \cdot T_f$), the sampling index j starts from 0 and increases up to $n_i - 1$ in (8).

A representation of output sampling from a series of grinding cycles is given in the discrete time domain as follows:

- **Within the ith cycle or when $j \in \{0, 1, \ldots, n_i - 1\}$:**

$$\begin{aligned}\mathbf{y}(i, j) &= \mathbf{y}_f \\ &= \mathbf{H}_f\left[\mathbf{X}(i, j), \mathbf{u}(i, j)\right] + \boldsymbol{\xi}_f(i, j)\end{aligned} \tag{9}$$

  where $\mathbf{H}_f$ is composed of the elements in $\mathbf{H}$ corresponding to the sensor output vector $\mathbf{y}_f$, and $\boldsymbol{\xi}_f(i, j)$ is the measurement noise (with covariance $\mathbf{R}_f$) in the sensor output.
- **At the end of the ith cycle or when $j = n_i$**

$$\mathbf{y}(i, n_i) = \mathbf{H}\left[\mathbf{X}(i, n_i), \mathbf{u}(i, n_i)\right] + \boldsymbol{\xi}(i, n_i) \tag{10}$$

  where $\boldsymbol{\xi}(i, n_i)$ is the measurement noise (with covariance $\mathbf{R}$) in the whole output including the sensor output. Both the slow and fast measurements are sampled at the end of the ith cycle.

III. OBSERVABILITY TEST

The observability was tested by linearizing the augmented model in (6) and (7) around more than ten operating points that were randomly selected from a typical trajectory such as the one described in Section IV. Table I summarizes the observability test for two estimation tasks, each with two measurement settings. Among the available measurements, the grinding power P and part-size reduction D_w are assumed to be measured with in-process sensors, whereas the wheel diameter d_s and surface roughness R_a would be obtained via postprocess inspection.

The first task in Table I is to estimate the state variables while excluding any model parameters (i.e., $\mathbf{X} = \mathbf{x}$). It can be seen from the first measurement setting of the task that the system is not observable when both P and D_w are measured. The estimation becomes feasible when d_s is directly measured in addition to P, as shown for the second setting. The second case in Table I involves estimating the state variables in addition to a model parameter in the surface roughness model, R_0, that is, $\mathbf{X} = [\mathbf{x}; R_0]$. The output equation in Appendix A for R_a is repeated here for reference as follows:

TABLE II
NOMINAL VALUES OF MODEL PARAMETERS IN THE SIMULATION

d_w (mm)	d_{s_0} (mm)	s_0	s_1	K_s (N/mm)	δ	γ
70	50	49.6	0.08	2380	1	0.2
R_g	R_0	V_0' (mm^3/mm)	r_m	r_0	G_1	G
0.7	3	300	2.4	1	13	0.9

$$R_a = \left[R_g + (R_0 - R_g)\exp\left(-\frac{x_1}{V_0'}\right)\right]\left(\frac{\pi d_w x_2}{u_2}\right)^{\gamma}. \tag{11}$$

It is evident from Table I that estimation of R_0 requires a direct measurement of R_a. In fact, most parameters in the output equations related to part quality (e.g., surface roughness and roundness) can only be made observable through direct feedback, which may not be available during a cycle run. The observability analysis in this section provides a strong motivation for involving postprocess measurement data in the estimation of model parameters, as well as full observability of state variables.

IV. MULTIRATE ESTIMATION SCHEME

This section describes the proposed estimation scheme, which is based on extended Kalman filters (EKFs). An EKF operation consists of *a priori* and *a posteriori* updates at each sampling instant. The *a priori* update is made through a discrete-time simulation of the model, whereas the *a posteriori* update involves comparing the *a priori* estimate with the actual measurement. In the following descriptions, a vector with a hat ("$\hat{}$") denotes an estimate after an *a posteriori* update, whereas one with both a hat and a minus sign ("$\bar{}$") denotes an *a priori* estimate.

During a cycle run, $\mathbf{X}$ is estimated using an EKF based on measurement of $\mathbf{y}_f$, while $\mathbf{y}_s$ is estimated by substituting the estimate, $\hat{\mathbf{X}}$, the known input, $\mathbf{u}$, and a zero noise, $\boldsymbol{\xi} = 0$, into the output equation. Another EKF operation is applied at the end of each grinding cycle based on both the sensor output and the postprocess measurement, thereby improving the robustness of the overall estimation. The multirate EKF operations used in this paper are described in more detail in Appendix B. In a sense, the scheme proposed here is similar to the multirate filtering schemes in [8] and [9] for continuous processes in the process industry, where both frequent and infrequent measurement data are used to estimate state variables and model parameters. However, since a series of grinding cycles is not strictly continuous, special considerations related to the continuity of variables are required, as described below.

At the beginning of a cycle, the actual infeed rate $v(= x_2)$ must start from zero regardless of its last estimate in the preceding cycle, i.e., $\hat{x}_2^-(i, 0) = 0$. On the other hand, the accumulated removal $V_w'(= x_1)$ by its definition, as well as the wheel

TABLE III
PROCESS AND MEASUREMENT NOISES FOR THE SIMULATION

Case	Augmented state vector, **X**	Process noise, **Q**	Measurement setting		Measurement noise, **R**
			In-process sensors	Postprocess inspection	
A	$(x_1, x_2, x_3)^T$	$4 \times \text{diag}[0.01\ 10^{-9}\ 10^{-9}]$	P, D_w	-	diag[10000 0.0001]
			P	d_s	diag[10000 10^{-6}]
B	$(x_1, x_2, x_3, R_0)^T$	$4 \times \text{diag}[0.01\ 10^{-11}\ 10^{-9}\ 10^{-9}]$	P, D_w	d_s	diag[10000 0.0001 10^{-6}]
			P	d_s, R_a	diag[10000 10^{-6} 0.0001]

diameter $d_s(= x_3)$, should be continuous across cycles. Hence, their estimate should be also continuous as

$$\hat{x}_{1,3}^{-}(i,0) = \hat{x}_{1,3}(i-1, n_{i-1}) \tag{12}$$

where $x_{1,3}$ corresponds to either V_w' or d_s.

In contrast, model parameter $\boldsymbol{\theta}$ cannot be strictly continuous between any two cycles in a series due to inherent variations in the grinding process. The cycle-to-cycle variations in batch production are often modeled as random step changes of the process between cycles [10]. Assuming that the step variations are purely random, the estimate of the process parameter at the beginning of a cycle is initialized to its last estimate in the previous cycle as follows:

$$\hat{\boldsymbol{\theta}}^{-}(i,0) = \hat{\boldsymbol{\theta}}(i-1, n_{i-1}). \tag{13}$$

V. SIMULATIONS

Simulations were performed for the two estimation tasks whose observability was tested in Section III. The first case involved estimation of state variables, whereas the second case study involved simultaneous state and parameter estimation for compensating the model-process mismatch.

The simulated process data were generated using (8)–(10) when $T_f = 0.02$ s from ten consecutive cycles based on the nominal values of the model parameters listed in Table II, which were obtained from various studies that have involved the grinding of heat-treated steels with aluminum oxide wheels [5], [6], [11]–[13]. Although not required by the proposed scheme, an identical set of grinding conditions was applied to each of the ten cycles. Specifically, the wheel speed v_s and the work speed v_w were fixed at 37 m/s and 0.533 m/s, respectively, whereas the command infeed rate u was scheduled such that plunge grinding is performed in three distinct stages of roughing, finishing, and spark-out within 17 s (roughing: $u = 0.0254$ mm/s for $0 \le t < 9.5$ s, finishing: $u = 0.0020$ mm/s for $9.5 \le t < 13.3$ s, spark-out: $u = 0$ mm/s for $13.3 \le t < 17$ s). Readers are directed to [6] for a detailed description of a typical plunge grinding cycle. Appropriate process and measurement noises as listed in Table III were added during the simulation according to (8)–(10).

A. Estimation of Wheel Diameter

A real-time knowledge of the wheel diameter is essential for achieving a tight control of the workpiece dimension [6], but in-process sensing of the wheel diameter is difficult due to the high rotation speed of the grinding wheel and its abrasive action.

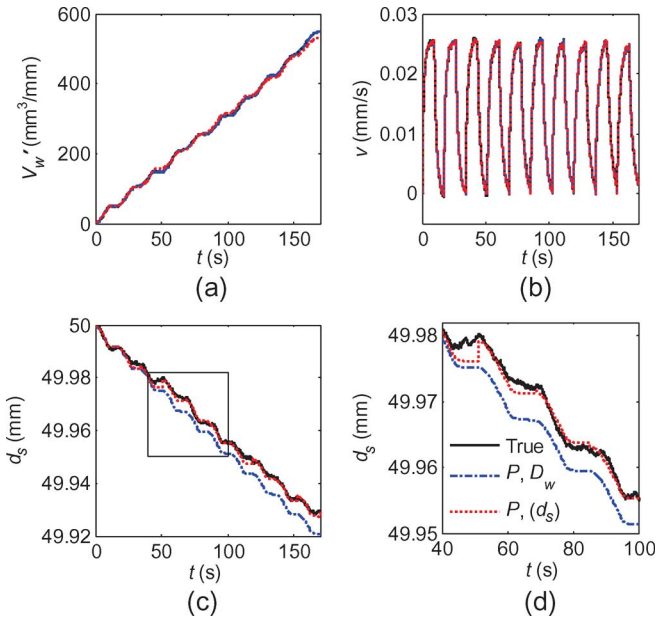

Fig. 3. Comparison of state estimation based on two measurement settings: $\mathbf{P}_0 = \text{diag}[10\ 10^{-7}\ 10^{-6}]$ and $\mathbf{Q} = 4 \times \text{diag}[0.01\ 10^{-9}\ 10^{-9}]$. The parentheses around d_s in the key denote that it is sampled through a postprocess measurement. (a) $V_w'(= x_1)$. (b) $v(= x_2)$. (c) $d_s(= x_3)$. (d) Magnified view of the plot within the rectangle in (c).

It is shown in Section III that the wheel diameter cannot be estimated based on measurement of either the grinding power P or the part-size reduction D_w. The main aim in this case study was to estimate the wheel diameter in real time during a cycle run through simulation of the process model based on input variables and estimates of other state variables, while intermittently correcting the estimate based on postprocess measurement of its actual value.

Fig. 3 compares the estimation results based on the two measurement settings with which the observability was tested as Case 1 in Table I. The initial error covariance is denoted as $\mathbf{P}_0$ in the figure caption along with $\mathbf{Q}$ denoting the process noise covariance for the extended Kalman filter. In the present study, covariance matrices of process noise and measurement noise for the Kalman filter were initially determined according to the simulation conditions listed in Table III and tuned by trial and error if necessary. In Fig. 3, the solid lines are the true values of the state variables, while the other two lines show estimates of the state variables based on the two measurement settings over a series of ten grinding cycles. Note that, for simplicity, Fig. 3 does not show any idle times between cycles associated with unloading and loading of parts.

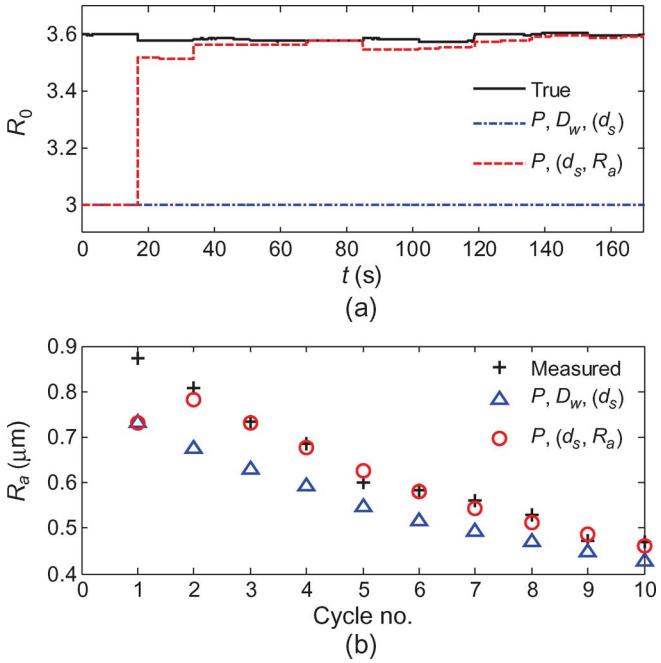

Fig. 4. Results of estimation: $\mathbf{P}_0 = \mathrm{diag}[0.1\ 10^{-11}\ 10^{-6}\ 0.01]$ and $\mathbf{Q} = 1.6 \times \mathrm{diag}[10^{-5}\ 10^{-14}\ 10^{-12}\ 10^{-7}]$. (a) Model parameter R_0. (b) Comparison of R_a and its *a priori* estimate $\hat{R}_A^-$ at the end of each cycle.

The first measurement setting corresponds to those of existing observers in studies based solely on in-process sensors [14]–[16]. Fig. 3 shows that, although the first two state variables were tracked well under both measurement settings, the estimated wheel diameter of the first measurement setting exhibits an offset from the true value. In contrast, correcting the estimate of the wheel diameter in the second measurement setting at the end of each grinding cycle leads to a better overall estimation.

B. Simultaneous State and Parameter Estimation for Surface Roughness

This case was a state-parameter estimation problem with a model-process mismatch in the output equation for the surface roughness. It is demonstrated that intermittent postprocess measurement of the part quality can reduce the model-process mismatch due to process variations as well as predict the part quality in real time.

In addition to the continuous drift described as the random walk process, both batch-to-batch variation and cycle-to-cycle variations were simulated for parameter R_0 in (11). A batch-to-batch variation was introduced by increasing R_0 by 20% from its value listed in Table II when the first cycle started, whereas a cycle-to-cycle variation was described as another random walk process by adding a white Gaussian noise with a covariance of 0.0001 to R_0 at the beginning of every cycle.

The estimation algorithm was applied to the simulated measurement data generated according to the above procedure, and input data. The performance of the proposed scheme in estimating R_0 as well as in predicting the surface roughness at the end of each grinding cycle is shown in Fig. 4. The true R_0 is shown as a solid line in Fig. 4(a), and the prediction in Fig. 4(b) refers to an *a priori* estimate of surface roughness at the end of each grinding cycle before an *a posteriori* update takes place based on measurement of the actual surface roughness. The measured surface roughness in Fig. 4(b) corresponds to that generated by simulation with a measurement error added according to (7).

Two measurement settings of Case 2 in Table I were considered in this case study. As expected from the results of the observability test, R_0 in the output equation for the surface roughness cannot be estimated based on the first measurement setting. On the other hand, R_0 was updated at the end of each cycle with the second measurement setting, as shown in Fig. 4(a), leading to a good agreement between the measured surface roughness and the prediction at the end of each cycle in Fig. 4(b).

VI. Conclusion

We have proposed a new control-oriented estimation scheme for a series of grinding cycles in the batch production of precision parts. Our analyses have revealed that active feedback of the postprocess measurement data allows new and effective observers to be developed, notably in cases where the grinding systems would be unobservable with existing in-process sensors. Although specific applications have been demonstrated for estimating problems in the grinding process, this paper has focused on introducing those involved in discrete machining in batches to the new concept of integrating all of the incoming data flows, with the aim of improving process control. A similar approach could be considered for machining processes in general, as well as polishing and chemical mechanical planarization operations for the optics and semiconductor industries.

Our future research is directed toward application of the estimation algorithm to other sensor outputs and part qualities (for which appropriate analytical models are not available in the literature) using neural networks. Convergence of the filter and systematic tuning of the initial error covariance $\mathbf{P}_0$ and the process noise covariance $\mathbf{Q}$ should also be investigated.

Appendix A
Examples of Output Equations

Some of the output equations can be obtained by substituting the state and input variables into previously reported analytical models as follows:

Grinding power [5], [7]:

$$P = K_s \left(s_0 + s_1 x_1^{\delta}\right) x_2.$$

Roundness [17]:

$$r = r_0 \frac{\pi d_w x_2}{v_w} + r_m.$$

Surface roughness [6], [18]:

$$R_a = \left[R_g + (R_0 - R_g)\exp\left(-\frac{x_1}{V_0'}\right)\right]\left(\frac{\pi d_w x_2}{u_2}\right)^{\gamma}.$$

The part-size reduction D_w and wheel diameter d_s directly correspond—by their definitions—to two of the state variables, i.e., $D_w = 2x_1/\pi d_w$ and $d_s = x_3$.

APPENDIX B
MULTIRATE EXTENDED KALMAN FILTER

The EKF operates in two distinct modes depending on the two sampling streams.

- **Within the ith cycle or when $j \in \{0,1,\ldots,n_i-1\}$**
  An *a priori* update takes place according to the discretized model in (8), while the error covariance $\mathbf{P}$ is updated according to the following equation:

$$\mathbf{P}^{-}(i,j) = \mathbf{A}(i,j-1)\mathbf{P}(i,j-1)\mathbf{A}^{\mathrm{T}}(i,j-1) + \mathbf{Q} \quad (14)$$

  where $\mathbf{A}$ is the Jacobian matrix of $\mathbf{F}_d$ with respect to $\mathbf{X}$. Once an *a priori* estimate of the sensor output, $\hat{\mathbf{y}}_f^{-}$, is calculated from (9) with zero noise, the *a posteriori* update is performed based on its difference from the actual sensor output $\mathbf{y}_f$ as

$$\hat{\mathbf{X}}(i,j) = \hat{\mathbf{X}}^{-}(i,j) + \mathbf{K}_f\left[\mathbf{y}_f(i,j) - \hat{\mathbf{y}}_f^{-}(i,j)\right] \quad (15)$$

$$\mathbf{P}(i,j) = \left[\mathbf{I} - \mathbf{K}_f\mathbf{C}_f(i,j)\right]\mathbf{P}^{-}(i,j) \quad (16)$$

  where $\mathbf{K}_f = \mathbf{P}^{-}(i,j)\mathbf{C}_f^{\mathrm{T}}(i,j)[\mathbf{C}_f(i,j)\mathbf{P}^{-}(i,j)\mathbf{C}_f^{\mathrm{T}}(i,j)+\mathbf{R}_f]^{-1}$ is the Kalman gain for the fast measurement, $\mathbf{C}_f(i,j)$ is the Jacobian matrix of $\mathbf{H}_f$ with respect to $\mathbf{X}$, and $\mathbf{R}_f$ is the covariance of the fast measurement noise, $\boldsymbol{\xi}_f$.
- **At the end of the ith cycle or when $j = n_i$**
  After the *a priori* state is estimated, an *a priori* estimate of the whole output, $\hat{\mathbf{y}}^{-}$ is calculated based on (10) with zero noise. Both the on-line sensor output and the off-line measurement data are used to update the state estimation as follows:

$$\hat{\mathbf{X}}(i,n_i) = \hat{\mathbf{X}}^{-}(i,n_i) + \mathbf{K}\left[\mathbf{y}(i,n_i) - \hat{\mathbf{y}}^{-}(i,n_i)\right] \quad (17)$$

$$\mathbf{P}(i,n_i) = \left[\mathbf{I} - \mathbf{K}\mathbf{C}(i,n_i)\right]\mathbf{P}^{-}(i,n_i) \quad (18)$$

  where $\mathbf{K} = \mathbf{P}^{-}(i,n_i)\mathbf{C}^{\mathrm{T}}(i,n_i)[\mathbf{C}(i,n_i)\mathbf{P}^{-}(i,n_i)\mathbf{C}^{\mathrm{T}}(i,n_i)+\mathbf{R}]^{-1}$ is the Kalman gain and $\mathbf{C}(i,n_i)$ is the Jacobian matrix of $\mathbf{H}$ with respect to $\mathbf{X}$, and $\mathbf{R}$ is the covariance of the measurement noise, $\boldsymbol{\xi}$.

ACKNOWLEDGMENT

The author would like to thank the three anonymous reviewers for their useful comments and suggestions.

REFERENCES

[1] S. Y. Liang, R. L. Hecker, and R. G. Landers, "Machining process monitoring and control: The state-of-the-art," *ASME J. Manuf. Sci. Eng.*, vol. 126, pp. 297–310, 2004.
[2] C. W. Lee, "A new dynamic state space model for the cylindrical grinding process," in *Proc. Int. Mech. Eng. Congr. Expo.*, Orlando, FL, Nov. 2005, vol. DSC-74, pp. 697–703.
[3] K. Danai and A. G. Ulsoy, "A dynamic state model for on-line tool wear estimation in turning," *ASME J. Eng. Ind.*, vol. 109, pp. 396–399, 1987.
[4] S. Elanayar and Y. C. Shin, "Robust tool wear estimation with radial basis function networks," *ASME J. Dyn. Syst., Meas., Contr.*, vol. 117, pp. 459–467, 1995.
[5] H. K. Tönshoff, T. Friemuth, and J. C. Becker, "Process monitoring in grinding," in *Proc. CIRP*, 2002, vol. 51, no. 2, pp. 551–571.
[6] S. Malkin, *Grinding Technology: Theory and Application of Machining With Abrasives*. Reading, MI: Soc. Manuf. Eng., 1989.
[7] R. I. King and R. S. Hahn, *Handbook of Modern Grinding Technology*. Reading, NY: Chapman and Hall, 1986.
[8] R. D. Gudi, S. L. Shah, and M. R. Gray, "Adaptive multirate state and parameter estimation strategies with application to a bioreactor," *AIChE J.*, vol. 41, no. 11, pp. 2451–2464, 1995.
[9] V. Prasad, M. Schley, L. P. Russo, and B. W. Bequette, "Product property and production rate control of styrene polymerization," *J. Process. Control*, vol. 12, pp. 353–372, 2002.
[10] W. Jang, "A new inspection sampling plan under capacity constraints and multiple shifts," *Int. J. Prod. Res.*, vol. 41, no. 6, pp. 1333–1345, 2003.
[11] C. W. Lee and Y. C. Shin, "Improved generalized intelligent grinding advisory system," in *Proc. Int. Mech. Eng. Congr. Expo.*, 1999, vol. MED-10, pp. 473–480.
[12] R. P. Lindsay, "The effect of wheel wear rate on the grinding performance of three wheel grades," in *Proc. CIRP*, 1983, vol. 32, no. 1, pp. 247–249.
[13] G. Xiao, S. Malkin, and K. Danai, "Intelligent control of cylindrical plunge grinding," in *Proc. ACC*, Chicago, IL, Jun. 1992, pp. 391–398.
[14] Y. Gao and B. Jones, "Fast time constant estimation for plunge grinding process control," *Int. J. Mach. Tools Manuf.*, vol. 39, pp. 143–156, 1999.
[15] D. A. Thomas, D. R. Allanson, J. L. Moruzzi, and W. B. Rowe, "In-process identification of system time constant for the adaptive control of grinding," *ASME J. Eng. Industry*, vol. 117, pp. 194–201, 1995.
[16] H. E. Jenkins and T. R. Kurfess, "Adaptive pole–zero cancellation in grinding force control," *IEEE Trans. Control Syst. Technol.*, vol. 7, no. 3, pp. 363–370, May 1999.
[17] S. Dong, K. Danai, S. Malkin, and A. Deshmukh, "Continuous optimal infeed control for cylindrical plunge grinding. Part 1: Methodology," *ASME J. Manuf. Sci. Eng.*, vol. 126, pp. 327–333, 2004.
[18] C. W. Lee, T. Choi, and Y. C. Shin, "Intelligent model-based optimization of the surface grinding process for heat-treated 4140 steel alloys with aluminum oxide grinding wheels," *ASME J. Manuf. Sci. Eng.*, vol. 125, no. 1, pp. 65–76, 2003.